

CO₂ fertilization of *Sphagnum* peat mosses is modulated by water table level and other environmental factors

Henrik Serk¹, Mats Nilsson², João Figueira³, Thomas Wieloch¹, and Juergen Schleucher¹

¹Umeå Universitet Medicinska fakulteten

²Sveriges Lantbruksuniversitet Fakulteten för Skogsvetenskap

³Umeå Universitet Teknisk-Naturvetenskaplig Fakultet

August 6, 2020

Abstract

Sphagnum mosses account for most accumulated dead organic matter in peatlands. Therefore, understanding their responses to increasing atmospheric CO₂ is needed for estimating peatland C balances under climate change. A key process is photorespiration: a major determinant of net photosynthetic C assimilation that depends on the CO₂ to O₂ ratio. We used climate chambers to investigate photorespiratory responses of *Sphagnum fuscum* hummocks to recent increases in atmospheric CO₂ (from 280 to 400 ppm) under different water table, temperature, and light intensity levels. We tested the photorespiratory variability using a novel method based on deuterium isotopomers (D6^S/D6^R ratio) of photosynthetic glucose. The effect of elevated CO₂ on photorespiration was highly dependent on water table. At low water table (-20 cm), elevated CO₂ suppressed photorespiration relative to C assimilation, thus substantially increasing the net primary production potential. In contrast, a high water table (~0 cm) favored photorespiration and abolished this CO₂ effect. The response was further tested for *Sphagnum majus* lawns at typical water table levels (~0 and -7 cm), revealing no effect of CO₂ under those conditions. Our results indicate that only hummocks, which typically experience low water table levels, benefit from the 20th century's increase in atmospheric CO₂.

INTRODUCTION

Only 3% of the earth's land surface is covered by peatlands, but more than a third of global soil carbon (C) is stored in boreal mires (Frolking *et al.* , 2011; Loisel *et al.* , 2014). Most of those mires are dominated by *Sphagnum* peat mosses, which hence contribute substantially to global peatland C sequestration (Gunnarsson, 2005; Wu *et al.* , 2012; Laing *et al.* , 2014; Loisel *et al.* , 2014). Thus, reliable prediction of future C sequestration and storage in peatlands requires profound understanding of *Sphagnum* C acquisition and accumulation (Frolking *et al.* , 2011; Charman *et al.* , 2013; Loisel, *et al.* , 2014; Wu & Roulet 2014), but the mosses' responses to increases in atmospheric CO₂ concentrations are still not well understood.

Sphagnum physiology strongly depends on local environmental conditions, including local weather, hydrology and nutritional constraints. Distinct *Sphagnum* species favor specific mire microhabitats, and form associated structures, including hummocks, lawns and hollows that reflect characteristic average water table (WT) levels (Rydin *et al.* , 2006; Weston *et al.* , 2015; Moor *et al.* , 2017; Nijp *et al.* , 2017). Key elements of the species' adaptation to these microhabitats are based on physiological and anatomical traits that govern their capillary water retention (Rydin & Clymo, 1989; McCarter & Price, 2014; Weston *et al.* , 2015). *Sphagnum fuscum* is an abundant globally distributed hummock species (Klinggräff, 1872) that is capable of growing up to 50 cm above the WT (Hogg, 1993; Gunnarsson, 2005; Rydin *et al.* , 2006). In contrast, *Sphagnum majus* inhabits lawns and hollows and grows generally less than 10 cm above the WT (Nijp *et al.* , 2014).

The ongoing increase in atmospheric CO₂ from preindustrial levels of 280 ppm to the contemporary ~400

ppm and concomitant changes in climate, such as higher temperatures and precipitation in the northern hemisphere, are expected to have major consequences for mire vegetation and C sequestration (Hilbert *et al.* , 2000; Belyea & Malmer, 2004; Limpens *et al.* , 2008; Froking *et al.* , 2011; Gallego-Sala *et al.* , 2018). CO₂ ‘fertilization’ on higher plants has been extensively studied, but its magnitude and underlying mechanisms remain unclear (IPCC, 2013; Ainsworth & Long, 2005; DeLucia *et al.* , 2005; Schimel *et al.* , 2015). Even less is known about *Sphagnum* mosses, which lack certain anatomical features of higher plants, such as the cuticle, stomata and roots, so they can only regulate CO₂ and water fluxes indirectly (Hayward & Clymo, 1982; Williams & Flanagan, 1998; Price & Whittington, 2010).

In previous manipulation experiments, conflicting results have been obtained concerning the photosynthetic response of *Sphagnum* to increases in atmospheric CO₂ levels. They found enhanced net photosynthesis, but not biomass, of *S. fuscum* (Jauhiainen *et al.* , 1994; Jauhiainen & Solviola, 1999). Most studies of other *Sphagnum* species also did not detect any increase in biomass (Van der Heijden *et al.* , 2000b; Berendse *et al.* , 2001; Heijmans *et al.* , 2001, 2002; Mitchell *et al.* , 2002; Toet *et al.* , 2006), except for Van der Heijden *et al.* (2000a). However, in most of these studies, effects of confounding factors such as temperature, moisture, light intensity and nutrient availability may have masked effects of changes in atmospheric CO₂ levels on C assimilation.

On the molecular level, C assimilation in C₃ plants such as *Sphagnum* is initiated by the reaction of CO₂ with ribulose 1,5-bisphosphate (RuBP, carboxylation), catalyzed by the enzyme Rubisco. Due to Rubisco’s enzymatic properties, this reaction is accompanied by a massive side reaction of RuBP with O₂ (oxygenation). This process gives rise to the photorespiration pathway, which leads to loss of C as CO₂; therefore, this oxygenation reaction decreases net CO₂ fixation (Laing *et al.* , 1974). Models predict that the anthropogenic increase in atmospheric CO₂ (from 280 to over 400 ppm) will generally result in suppressed C₃ photorespiration rates (under given conditions) and contribute to an increase in net photosynthesis of ~35% (Ehlers *et al.* , 2015). Thus, robust understanding of the ratio of photorespiration to gross photosynthesis and its determinants is crucial for predicting overall net C balances of terrestrial biomass, and particularly for modeling responses of photosynthetic processes to changes in environmental conditions (Weston *et al.* , 2015; Pugh *et al.* , 2016).

The above-mentioned conflicting responses in *Sphagnum* C assimilation were observed in manipulation experiments, with CO₂ increases above ambient (> 350 ppm). Another question is how to constrain the response that has occurred over the 20th century. To date there are no methods to trace if there has been a suppression of photorespiration during the 20th century. However, accurate estimates of the ratio of photorespiration to gross photosynthesis, at the time of formation of both current and historical plant tissues, can be obtained using deuterium (D) isotopomers (Ehlers *et al.* , 2015). In this method, the abundance ratio of the D isotopomers named D6^S and D6^R in the C₆H₂ group of glucose derived from hydrolyzed cell wall carbohydrates is measured by NMR spectroscopy (Fig. 1).

The D6^S /D6^R ratio indicates the Rubisco oxygenation to carboxylation flux ratio, and thus the photorespiration to gross photosynthesis ratio. For simplicity, in the following text we will refer to this ratio as photorespiration/photosynthesis ratio. Analysis with this method confirmed that the photorespiration of many C₃ plants was suppressed and their net photosynthesis rates increased by the last century’s increase in atmospheric CO₂ (Ehlers *et al.* , 2015). In the cited study, comparison of *S. fuscum* herbarium material formed at [?] 300 ppm atmospheric CO₂ with modern plants showed that net photosynthesis rates of peat-forming *Sphagnum* also increased during the last century. However, the extent to which photorespiration of *Sphagnum* plants is suppressed at increased atmospheric CO₂ may be influenced by other factors, particularly water content, temperature and light intensity. Thus, the overall aim was to understand variations and potential effect of suppressed photorespiration (and associated changes in C assimilation rates) in relation to biogeophysical conditions at peatland surfaces and climatic changes. This will allow us to explain D isotopomer data of historical *Sphagnum* tissues. To address this aim, we investigated the response of *S. fuscum*’s photorespiration/photosynthesis ratio to the recent increase in atmospheric CO₂ under various combinations of different atmospheric CO₂, WT, temperature and light intensity levels. To do so, we used

D isotopomers as well as $\delta^{13}\text{C}$, $\delta^{15}\text{N}$ and elemental analysis (C and N). The response was further tested for the lawn species *S. majus* at different CO_2 and WT levels.

MATERIALS AND METHODS

Plant material

Peat mesocosms from hummocks dominated by *Sphagnum fuscum* (Schimp.) Klinggr. and lawns dominated by *Sphagnum majus* (Russ.) Jens. were collected in May and August of 2016, and July 2017, from the same site located at the northern end of the Degerö-Stormyr peatland. Degerö-Stormyr is a nutrient-poor minerogenic mire in northern Sweden (64°11'N, 19°33'E, 270 m asl) near Vindeln municipality that is included in the ICOS (Integrated Carbon Observation System; Franz *et al.*, 2018) Swedish national and European research infrastructure. Mesocosms of 20 x 20 x 25 cm were collected using a sharp knife and transferred to 11 L square plastic containers for subsequent incubation in climate-controlled growth chambers. Vascular plants (*Andromeda polifolia*, *Rubus chamaemorus*, *Vaccinium oxycoccus*, *Drosera rotundifolia*, *Empetrum nigrum*, *Scheuchzeria palustris*, *Eriophorum vaginatum* and *Carex spp.*) and *Polytrichum* spp. mosses were removed before incubation.

Manipulation experiments

Triplicate mesocosms were grown in climate-controlled growth chambers (PGC-7L2/DE, Percival Scientific, USA) at Umeå Plant Science Centre for 8-10 weeks with 18/6-h day/night photoperiods and 70% relative humidity (corresponding to average growing season photoperiods and humidity conditions at Degerö-Stormyr: www.icos-sweden.se) under different CO_2 concentrations and WT levels. Two identical chambers were used for incubation at atmospheric CO_2 concentrations of 280 ppm and 400 ppm, respectively with two different WT levels (hummocks: 0 and -20 cm, lawns: 0 and -7 cm below capitulum) in each chamber. CO_2 levels in the growth chambers were regulated automatically, solely by removal. Thus, the CO_2 in the chambers derived from the atmosphere. Target WT levels were obtained by placing the 11 L plastic containers in larger plastic storage containers, which were then filled with deionized water to the target WT level (Fig. S1). The WT was re-adjusted every 2 days, resulting in variations of ± 2 cm. Mesocosms incubated at low WT were sprayed with deionized water every 2 days to maintain the high moisture levels that are naturally provided in the mire by precipitation.

The above-mentioned incubations were conducted in three batches with different temperature and light intensity settings. The first two batches were performed at light intensities of $250 \mu\text{mol m}^{-2}\text{s}^{-1}$ (at moss surface) and day/night temperatures of either 12°C/7°C or 17°C/12°C, whereas the last batch was conducted at $500 \mu\text{mol m}^{-2}\text{s}^{-1}$ and 17°C/12°C. Thus, the first two incubations represent a full 2^3 factorial design with low light intensity as a fixed factor and atmospheric CO_2 concentration, WT and temperature as variables, and the last incubation a 2^2 factorial design, with temperature and light intensity as fixed factors and CO_2 concentration and WT as variables. In the following text, the different CO_2 , WT, temperature and light settings are referred to as low and high levels respectively. The temperature settings were chosen according to typical growth-period conditions in the field (Peichl *et al.*, 2014). Light intensity settings were chosen in the range of typical *Sphagnum* light saturation ($250\text{--}500 \mu\text{mol m}^{-2}\text{s}^{-1}$; Harley *et al.*, 1989; Jauhainen & Solviola, 1999; Laine *et al.*, 2011). The response variables measured in the experiments were: photorespiration/photosynthesis ratio ($\text{D}_6^{\text{S}}/\text{D}_6^{\text{R}}$ ratio), moss height increment, biomass production, ^{13}C and ^{15}N discrimination, and concentrations of C and N in the plant tissue.

Biomass and height increment measurements

Height increments of the moss in the mesocosms were measured weekly during the incubation period (Fig. S2), using five brush wires (Rydin & Jeglum, 2013) inserted into each mesocosm container. At the end of the incubation period, biomass formed during the incubation was harvested by cutting the moss at its initial height (essentially its capitulum), based on the brush wire data. Its fresh weight was determined and the material was dried at 60°C for 48 h to determine the dry weight and subsequently the water content of the moss. The biomass production of each replicate (moss in each container) was estimated by dividing

the dry weight of each replicate obtained after harvest, by its surface area (calculated based on container dimensions) and incubation time. Biomass density was calculated by dividing the dry weight of each replicate by its surface area and total height increment.

Sample preparation for D isotopomer measurements

Dry moss biomass formed during the incubations was ground to a fine powder at 30 Hz for 2 min using a MM 400 ball mill (Retsch®, Haan, Germany), and 200-700 mg portions were used as starting material for the following sample preparation for D isotopomer measurements. Glucose-containing structural polymers were hydrolyzed to glucose and converted to 1,2-O-isopropylidene- α -D-glucofuranose according to established protocols (Betson *et al.*, 2006). To remove contamination by a mannose derivative, which has overlapping signals with the NMR spectrum of the glucose derivative, an oxidation step was introduced. Each sample was dissolved in 20 mL 0.187 M phosphate buffer (NaH_2PO_4 , pH 4), 15.6 mg NaClO_2 was added per 100 mg sample and the pH was adjusted to 3.5 with H_3PO_4 . The NaClO_2 addition and pH adjustment was repeated five times over a period of 3 days (every 12 h). The complete reaction procedure was performed under the absence of light. 12 h after the last addition the reaction was quenched by adding a molar equivalent amount of Na_2SO_3 to the total amount of NaClO_2 added, then the mixture was neutralized with CaCO_3 , vacuum-filtered and evaporated under reduced pressure. To remove remaining salts the sample was extracted three times with 20 mL ethanol. The derivative was subsequently converted to 3,6-anhydro-1,2-O-isopropylidene- α -D-glucofuranose following Schleucher *et al.* (1999). The derivative was purified by flash chromatography using silica gel and diethyl ether. Pure fractions were identified by thin-layer-chromatography and pooled. Diethyl ether was evaporated, the sample was washed with amylene-stabilized chloroform and purity was checked by ^1H -NMR.

D isotopomer quantification

For NMR measurements of intramolecular D abundances, each sample of the glucose derivative, prepared as described above, was dissolved in a mixture of 83% v/v acetonitrile, 17% C_6F_6 and 0.01% C_6D_6 then transferred to a 5-mm NMR tube with a PTFE valve (J. Young Scientific Glassware Ltd., Windsor, U.K.) containing ~5 mg of NaHCO_3 . D-NMR measurements were acquired and processed as described by Betson *et al.* (2006) using an AVANCE III 850 spectrometer (Bruker BioSpin GmbH, Rheinstetten, Germany) equipped with a ^{19}F lock and a cryogenic probe optimized for D detection. D-NMR spectra were integrated by deconvolution with a Lorentzian line shape fit, using TopSpin™ 3.2 (Bruker BioSpin GmbH, Rheinstetten, Germany). The $\text{D6}^S/\text{D6}^R$ isotopomer ratio was determined as the ratio of the integrals of the D6^S and D6^R signals (Fig. 1). For each sample, five to eight spectra were recorded and the average of the $\text{D6}^S/\text{D6}^R$ ratios was calculated.

C and N-isotope and elemental analysis

C and N isotopic signatures ($\delta^{13}\text{C}$ and $\delta^{15}\text{N}$, respectively) and C and N contents of dry samples of moss tissues (ca. 5 mg) were analyzed via conversion to CO_2 and N_2 by combustion and quantification by mass spectrometry (Werner *et al.*, 1999), using a DeltaV isotope ratio mass spectrometer (Thermo Fisher Scientific, Bremen, Germany). The data were corrected for drift and non-linear sample size effects. For quantification, we used laboratory standards consisting of wheat and maize flours calibrated against certified reference standards: cyclohexanone, nicotinamide, and sucrose for C; atropine, cellulose, and NIST 1515 apple leaves for N; IAEA-600, IAEA-CH-6, and USGS40 for $\delta^{13}\text{C}$; and IAEA-600, IAEA-N-2, USGS40, and USGS41 for $\delta^{15}\text{N}$.

Calculation of chloroplastic CO_2 concentrations

Chloroplastic CO_2 concentrations (c_c) were calculated based on $\delta^{13}\text{C}$ signatures of the moss ($\delta^{13}\text{C}_{\text{moss}}$), using equations published by Flanagan & Farquhar (2014), with modifications to account for the lack of

stomatal resistance in *Sphagnum* :

$$^{13}\text{C}_{\text{moss}} = 1000 \frac{\delta^{13}\text{C}_{\text{atm}} - \delta^{13}\text{C}_{\text{moss}}}{1000 + \delta^{13}\text{C}_{\text{moss}}} \quad \delta^{13}\text{C}_{\text{moss}} = a_m \left(\frac{c_a - c_c}{c_a} \right) + b \left(\frac{c_c}{c_a} \right) - f \left(\frac{\Gamma^*}{c_a} \right) \quad n$$

Here, $\delta^{13}\text{C}_{\text{atm}}$ is the $\delta^{13}\text{C}$ signature of atmospheric CO_2 (-8.5‰), the fractionation during CO_2 diffusion through water to the chloroplast (1.8, 1989), b the discrimination during carboxylation by Rubisco (29photorespiration (16.2‰ the CO_2 compensation point ($\mu\text{mol mol}^{-1}$) in the absence of dark respiration (calculated from the temperature response: $\Gamma^* = 42.7 + 1.68 (T - 25) + 0.0012 (T - 25)^2$, where T is temperature in $^{\circ}\text{C}$; Brooks & Farquhar, 1985). When applying this equation we assumed, following Evans & von Caemmerer (2013), that no fractionation occurred during day respiration.

Statistical analysis

Effects of the varied environmental factors on the measured physiological parameters were assessed by ANOVA, implemented in R (version 3.6.1, RStudio, Inc.), using linear regression models. Three- and four-way interactions were not included in the models to prevent overfitting and to improve interpretability of the models. To compute the ANOVA with type II sum of squares, we used the *Anova* () function of the *car* package. The models were optimized for a better tradeoff between fit and complexity by applying automated stepwise model selection based on Akaike's information criterion using the *step* () function of the *stats* package with default settings (Venables & Ripley, 2002). Post-hoc Fisher's LSD tests with Benjamini-Hochberg correction (Benjamini & Hochberg, 1995; Steelet al., 1997) were applied, using the *LSD.test* () function, to account for false discovery rates. Microsoft Excel was used for all other data analysis.

RESULTS

Photorespiration response and biomass production

The two most important factors explaining the variation in the $\text{D6}^{\text{S}}/\text{D6}^{\text{R}}$ ratio (range: 0.85-0.94) were WT and atmospheric CO_2 concentration, which respectively accounted for 48% ($P < 0.001$) and 14% ($P < 0.001$) of the total variance (Fig. 2A, Table 1). In addition, temperature and interactions between WT and CO_2 both explained 7% each ($P = 0.004$ and $P = 0.005$, respectively) of the variance in this ratio. Increasing atmospheric CO_2 from 280 to 400 ppm resulted in a 0.03 decrease in the $\text{D6}^{\text{S}}/\text{D6}^{\text{R}}$ ratio at low WT, but had no significant effect on it at high WT (Fig. 2A, Table S1). Together with the observed interaction between CO_2 and WT, this indicates WT-dependent suppression of photorespiration at the high CO_2 level. Raising the WT from -20 to ~0 cm resulted in a significant (0.01-0.05) increase in the $\text{D6}^{\text{S}}/\text{D6}^{\text{R}}$ ratio, indicating that the high WT increased the photorespiration/photosynthesis ratio (Fig. 2A). Increasing the day/night temperatures from 12@C/7@C to 17@C/12@C caused a small (~0.01) increase in the $\text{D6}^{\text{S}}/\text{D6}^{\text{R}}$ ratio at low WT, but increasing the light intensity from 250 to 500 $\mu\text{mol m}^{-2} \text{s}^{-1}$ had no significant effect on it (Fig. 2A, Table 1).

Theoretically, the suppression of photorespiration at high CO_2 and low WT should have been accompanied by increases in CO_2 assimilation rates, and thus biomass production, but no significant increase in biomass accumulation associated with the high CO_2 level was observed under any test conditions (Fig. 2B). The variation in biomass production (0.2-3.6 $\text{g m}^{-2} \text{d}^{-1}$) was mostly explained by temperature (27%, $P < 0.001$), WT (52%, $P < 0.001$), and to a smaller degree light intensity (4%, $P = 0.003$) and the interaction between temperature and WT (4%, $P = 0.005$; Table 1). Increasing the temperature caused a massive 2.6- to 4.5-fold increase in biomass production, whereas raising the WT strongly reduced biomass production, by 53-74% (Fig. 2B). Increasing the light intensity caused a 1.1- to 1.5-fold increase in biomass. No major between-differences in C content of the biomass ($48.1 \pm 0.11\%$, SE) were detected (Fig. S3). Thus, the observed changes in biomass production reflect proportional variations in C accumulation.

Ωηολε-τισσσε δ¹³α ανδ ζηλοροπλαστis το αμβιεντ ¹⁸O₂ ρονςεντρατιον

To further investigate physiological effects of increasing atmospheric CO₂ from 280 to 400 ppm, we analyzed ¹³C discrimination by measuring whole-tissue ¹³C signatures (Fig. 3A). Variation in ¹³C (which ranged from -30.5 to -25.7‰ by changes in WT (48%, $P < 0.001$), atmospheric CO₂ (13%, $P < 0.001$), temperature (10%, $P < 0.001$), light intensity (3%, $P = 0.02$), and the interaction between CO₂ and WT (10%, $P < 0.001$; Table 1). Increasing atmospheric CO₂ consistently decreased ¹³C (by 1.4 to 1.7 ‰ 3A, Table S1). Concomitantly, raising the WT resulted in a 0.5-2.5‰ increase in ¹³C. Increasing the temperature caused a significant, 0.5-1.0 ‰ the light intensity resulted in a small 0.3-0.6‰ ¹³C at low WT.

The ¹³C data allowed estimation of the chloroplastic CO₂ concentration (c_c) and subsequently the chloroplastic to ambient CO₂ ratio (c_c/c_a , Flanagan & Farquhar, 2014), which is a key determinant of metabolic C fluxes. Variation in c_c/c_a (0.63-0.80, Fig. 3B) was explained by WT (57%, $P < 0.001$), light intensity (4%, $P = 0.022$), temperature (3%, $P = 0.035$), atmospheric CO₂ (3%, $P = 0.046$) and the interaction between CO₂ and WT (13%, $P < 0.001$; Table 1). Increasing atmospheric CO₂ significantly increased c_c/c_a , by 0.03-0.05, at low WT but had no significant effect at high WT (Fig. 3B, Table S1). Raising the WT caused a 0.02-0.09 decrease in c_c/c_a , and increasing the temperature decreased c_c/c_a by 0.02 at low WT. Altogether, this indicates that increases in atmospheric CO₂ increase c_c particularly at low WT, whereas raising the WT reduces c_c . A strong negative correlation was detected between c_c/c_a and the D6^S/D6^R ratio at low WT ($R^2 = 0.85$, $P < 0.001$), suggesting that an increase in c_c caused the decrease in photorespiration/photosynthesis ratio, i.e. suppression of photorespiration at low WT. No significant relationship in these variables was observed at high WT ($R^2 = 0.10$, $P = 0.208$).

Variation in the CO₂ diffusion gradient (72-150 ppm) from the atmosphere to the chloroplasts ($c_a - c_c$) was mostly explained by CO₂ (53%, $P < 0.001$), WT (26%, $P < 0.001$) and the interaction of CO₂ and WT (9%, $P < 0.001$). Increasing atmospheric CO₂ resulted in increases in $c_a - c_c$ of 15-52 ppm (Fig. S3, Table S2). This indicates that increases in atmospheric CO₂ increased CO₂ assimilation.

C/N ratio and nitrogen content

The lack of response of *S. fuscum* biomass production to high atmospheric CO₂ suggested biochemical limitations of the photosynthetic machinery. To explore the nature of possible limitations we investigated changes in whole-tissue N contents and C/N ratios (Fig. 3C, D). Variation in the C/N ratio (40-89 units) was mostly explained by WT (31%, $P < 0.001$), atmospheric CO₂ (12%, $P = 0.003$), interaction between temperature and WT (11%, $P = 0.004$), and interaction between CO₂ and WT (7%, $P = 0.022$, Table 1). Increasing the atmospheric CO₂ concentration increased the tissue C/N ratio by 4 to 23 units at low WT, but had no significant effect at high WT (Fig. 3C, Table S1). Increasing the WT generally decreased the C/N ratio by 5 to 31 units. The changes in C/N ratio were primarily due to changes in tissue N content, the C content only showed minor variation (Fig. S3).

Accordingly, the total variation in N content (5.5-11.8 mg g⁻¹) was explained by WT (31%, $P < 0.001$), atmospheric CO₂ (11%, $P = 0.013$) and the interaction between WT and temperature (8%, $P = 0.031$, Table 1). Increasing the CO₂ level decreased the N content by 7-28 % at low WT, but had no significant effect at high WT (Fig. 3D, Table S1). Increasing the WT caused a 1.1- to 1.6-fold increase in N content. Both C/N ratio and N content were strongly correlated with the D6^S/D6^R ratio at low WT ($R^2 = 0.68$, $P < 0.001$ and $R^2 = 0.71$, $P < 0.001$, respectively). At high WT the ratio was still correlated, but less strongly, with both the C/N ratio ($R^2 = 0.44$, $P < 0.003$) and N content ($R^2 = 0.40$, $P < 0.005$).

No major between-treatment differences were detected in whole-tissue ¹⁵N signatures (average: -3.63 ± 0.08 ‰). According to the 4-way ANOVA, the only significant effect was a small (~ 0.45 ‰) intensity ($R^2 = 0.23$, $P = 0.003$, Table S2).

Biomass density, height increment and water content

For further assessment of possible morphological effects of observed responses to increasing atmospheric CO₂ on *S. fuscum*, we measured its biomass density (total biomass dry weight per volume) and height increment under all the test conditions (Fig. 3E, F). No effect of atmospheric CO₂ on biomass density was observed,

instead the variation in density (4.1 to 42.4 g dm⁻³) was mostly explained by WT (45%, $P < 0.001$), light intensity (34%, $P < 0.001$) and the interaction between WT and light (14%, $P < 0.001$, Table 1). Raising the WT decreased biomass density by 41-71%, whereas light intensity increased it 2.1- to 3.5-fold at low WT and 1.6- to 2.6-fold at high WT (Fig. 3E).

Most of the variation in height increment (0.04-0.26 mm d⁻¹) was explained by temperature (51%, $P < 0.001$) and light intensity (24%, $P < 0.001$), while the interactions between light and WT or CO₂ as well as temperature and WT or CO₂ made minor contributions (each 2-3%, $P < 0.05$, Table 1). Increasing the temperature increased the height increment 2.4- to 4.5-fold (Fig. 3F), while increasing the light intensity resulted in ~0.6- and ~0.35-fold reductions in the height increment at low and high WT, respectively. Increasing atmospheric CO₂ significantly reduced height increment by 0.19 to 0.35-fold only at the high temperature and low light treatment, at low WT (Fig. 3F, Fig. S2).

S. fuscum 's water content was consistently 4-9 % lower at the high CO₂ level, but CO₂ only explained a small amount of the total variation (6.6-23.4 g g⁻¹) in its water content (1%, $P = 0.006$; Table S2, Fig. S3). Most of the variation was explained by WT (83%, $P < 0.001$), temperature (5%, $P < 0.001$), and the interactions between WT and temperature (6%, $P < 0.001$) and between WT and light (3%, $P < 0.001$, Table S2). At low WT, the water content varied between 7.4 and 10.6 g g⁻¹, within the reported optimal range for photosynthesis (6-10 g g⁻¹: Silvola & Aaltonen, 1984; Schipperges & Rydin, 1998). At high WT, the water content was between 15.4 and 22.3 g g⁻¹, far outside the optimal range for photosynthesis (Fig. S3).

Photorespiration response of *S. majus*

The observed CO₂-response of the D6^S /D6^R ratio of *S. fuscum* at high WT suggests that lawns and hollows, which generally experience relatively high WT levels, do not suppress photorespiration at high CO₂ levels. To test this, we analyzed D6^S /D6^R ratios of *S. majus* grown at different CO₂ and WT levels (under high temperature and low light conditions). Increasing CO₂ from 280 to 400 ppm did not have any significant effect on the D6^S /D6^R ratio (range: 0.90-0.98) of *S. majus* at both low (-7 cm) and high WT (~0 cm, $R^2 = 0.01$, $P = 0.153$, Table 2, Fig. 4A). In contrast, raising the WT resulted in a significant increase in the D6^S /D6^R ratio (0.05-0.06), indicating increased photorespiration/photosynthesis ratios at high WT levels ($R^2 = 0.94$, $P < 0.001$, Table 2). Biomass production did not show any significant difference in response to increasing atmospheric CO₂, but raising the WT reduced biomass production by ~40% ($R^2 = 0.49$, $P = 0.01$, Table 2, Fig. 4B). Elevated atmospheric CO₂ concentrations increased biomass density by 2-fold at low WT ($R^2 = 0.18$, $P = 0.048$, Table 2, Fig. 4C). Concomitantly, height increment significantly decreased at low WT by 55% ($R^2 = 0.5$, $P = 0.012$, Table 2, Fig. 4D, Fig. S2). The water content ranged between 9.1 and 11.9 g g⁻¹ at low WT and 10.8 and 17 g g⁻¹ at high WT, thus increasing the WT shifts the water content from optimal to suboptimal conditions for photosynthesis (Schipperges & Rydin, 1998). Altogether, these data indicate that despite optimal moisture conditions for photosynthesis, increasing atmospheric CO₂ does not affect C assimilation of *S. majus*.

DISCUSSION

Effects of increased atmospheric CO₂ on *S. fuscum* photosynthesis

The net photosynthesis rate of *S. fuscum*, as characterized by the D6^S /D6^R ratio, was significantly higher at the higher (current) atmospheric CO₂ level than at the lower (pre-industrial) level at low WT (Fig. 2A). D6^S /D6^R ratios were lower at the high CO₂ level when the WT was low (representing typical growth conditions for *S. fuscum*), thus indicating suppression of photorespiration relative to C assimilation during the 20th century. In contrast, when the *Sphagnum* plants were water-saturated, increasing atmospheric CO₂ from 280 to 400 ppm had no significant detected effects on their photosynthesis, *i.e.* on the D6^S /D6^R ratio. The observed shift in the D6^S /D6^R ratio of 0.03 units at low WT (Fig. 2A) is consistent with results of a previous comparison of contemporary samples with >100-year-old herbarium samples of *S. fuscum* (Ehlers *et al.*, 2015).

Of all tested environmental variables, the CO₂ concentration had the largest effect, explaining 53% of the

variance of $D6^S/D6^R$ under typical hydrological (low WT) conditions for *S. fuscum* (Table S1). Thus, our experimental data confirm that the detected suppression of photorespiration in herbarium samples (Ehlers *et al.*, 2015) was due to increases in atmospheric CO_2 during the last century. Estimates of c_c/c_a revealed an increase under contemporary CO_2 levels at low WT, and a high negative correlation with the $D6^S/D6^R$ ratio. This implies that the suppression of photorespiration derives from the higher intercellular CO_2 concentration suppressing Rubisco oxygenation. In line with the increase in c_c , the CO_2 diffusion gradient ($c_a - c_c$) was higher at the high CO_2 level than at the low CO_2 level when the WT was low, supporting the increase in CO_2 assimilation at the 400 ppm CO_2 level (Fig. S3).

Effect of moss water content

The increase in the $D6^S/D6^R$ ratio from low to high WT (Fig. 2A, 4A) revealed an increase in the photorespiration/photosynthesis ratio, and thus reduction in net photosynthesis at the high WT for both *S. fuscum* and *S. majus*. A concomitant decrease in c_c/c_a from low to high WT (Fig. 3B) suggests that the increase in the photorespiration/photosynthesis ratio was driven by a decline in c_c . In addition, the lower c_c/c_a at high WT is indicative of higher CO_2 diffusion resistance, resulting from the higher moss water content (Fig. S3). In this respect, our data supports the hypothesis that the higher water content at high WT limits CO_2 diffusion and therefore C assimilation. This hypothesis is also supported by earlier reports of reductions in net photosynthesis with increases in water content (Titus *et al.*, 1983; Titus & Wagner, 1984; Schipperges & Rydin, 1998) and a negative relationship between water content and c_c/c_a (Rice & Giles, 1996; Williams & Flanagan, 1996, 1998).

Limitations for *Sphagnum* biomass production

The lack of observed response of biomass production to increased atmospheric CO_2 (Fig. 2B) is consistent with findings of several other studies on different *Sphagnum* species (Jauhiainen *et al.*, 1994, 1998; Van der Heijden *et al.*, 2000b; Berendse *et al.*, 2001; Heijmans *et al.*, 2001, 2002; Mitchell *et al.*, 2002; Toet *et al.*, 2006). In contrast, the decrease in photorespiration/photosynthesis ratio we detected clearly indicates increased C assimilation (assuming constant RuBP turnover rates) and thus increased NPP potential in response to increased atmospheric CO_2 . At low WT, increasing the CO_2 level caused a slight but not significant increase in biomass production at high light, and a slight decrease at low light (Fig. 2B), suggesting that under field conditions, where light intensities are much higher, there might well be a CO_2 -driven increase in NPP. Thus, elevated CO_2 might shift the light saturation point even above 500 $\mu mol\ m^{-2}\ s^{-1}$ (Hajek *et al.*, 2009).

Furthermore, increases in atmospheric CO_2 may only enhance biomass production of higher C_3 plants if sufficient nutrients are available (Arp *et al.*, 1998; Poorter, 1998; Kirschbaum, 2011). Accordingly, we observed a decrease in *Sphagnum* tissue N content and an increase in the C/N ratio at elevated CO_2 (Fig. 3C, D), resulting in a high correlation with the $D6^S/D6^R$ ratio. In higher C_3 plants, acclimation to increased CO_2 levels has been found to reduce leaf N and Rubisco contents due to reductions in demand for Rubisco (Drake *et al.*, 1997; Cotrufo *et al.*, 1998). This indicates reduced N investment in Rubisco under elevated CO_2 and suggests that increasing CO_2 reduces Rubisco limitation of C assimilation (Fig. 2A, 3D). Reductions in N contents associated with increases in CO_2 , which suppress photorespiration, have been observed in several *Sphagnum* species including *S. fuscum*, *S. recurvum*, *S. palustre*, and *S. magellanicum* (Jauhiainen *et al.*, 1998; Van der Heijden *et al.*, 2000b; Toet *et al.*, 2006; Heijmans *et al.*, 2001). This suggests similar effects of elevated CO_2 on N content in most *Sphagnum* species.

Ecophysiological implications

Our results show that hummocks with characteristic WT levels have profited from CO_2 fertilization imposed by the 20th centuries CO_2 increase. The high WT conditions in this study resulted in abolishing the effect of CO_2 for both hummocks and lawns, demonstrating the importance of the water content for photosynthetic C fluxes. Even under optimal moisture conditions for photosynthesis (at WT of -7 cm), lawns did not respond to increased atmospheric CO_2 (Fig. 4A). Together with the observed response of *S. fuscum*, this suggests a species-specific suppression of photorespiration, which may be attributed to differences in leaf-anatomy

between hummock and lawn species (Rice & Giles, 1996). Thus, in contrast to hummock-species, certain lawn-species may not be capable of responding to changes in atmospheric CO₂.

Predicted increases in precipitation in the northern hemisphere are suggested to be compensated for by concomitant increases in evapotranspiration due to higher temperatures (Frolking *et al.*, 2011). This suggests that hydrological conditions of northern peatlands will remain relatively stable in a changing climate. Therefore, our data point towards changes in peatland topography in response to climate change, with the competitive advantage of hummocks over lawns and hollows.

Our results further indicate that for hummocks with typical WT conditions, the increase in atmospheric CO₂ during the 20th century was the major driver of *Sphagnum* photosynthetic C fluxes. During the early and mid-Holocene, atmospheric CO₂ was relatively stable, at ~270 ppm (Indermühle *et al.*, 1999), thus temperature appeared to control northern peatland C fluxes; peat C accumulation followed the increase in temperature during the early Holocene and the cooler and wetter climate during the neoglacial period (Yu *et al.*, 2009; Loisel *et al.*, 2014). Our results suggest that the ongoing increase in atmospheric CO₂ today, in marked contrast to its stability in the Holocene, has important consequences for peatland C fluxes.

CONCLUSION

Here we show that *S. fuscum*'s photorespiration is suppressed, *i.e.* net photosynthesis increased, in response to the last century's increase in atmospheric CO₂. This response was highly dependent on WT, with water-saturating conditions abolishing the CO₂ effect. Although those conditions are not typical for hummocks, they frequently occur for lawns. Lawns did not show any suppression of photorespiration, neither under water-saturation nor under optimal moisture conditions, suggesting a reduced CO₂ effect for those microhabitats. Variations in temperature and light intensity did not affect the extent of the CO₂-driven suppression of photorespiration. Our study revealed that D isotopomers are a valuable tool for understand metabolic C fluxes in *Sphagnum*. The results presented in this study will allow validation of D isotopomer analysis of peat archives and provide the basis for modelling global peatland C fluxes.

ACKNOWLEDGEMENT

The authors acknowledge the help provided by the 'NMR for Life' infrastructure supported by the Wallenberg Foundations, the SITES (Swedish Infrastructure for Ecosystem Science) and ICOS research infrastructures (for maintaining the Kulbäcksliden/Degerö Stormyr facility) funded by the Swedish research council (VR), the SciLifeLab infrastructure, the SLU Stable Isotope Laboratory (for C- and N-isotope and elemental analysis), Umeå Plant Science Center (for providing the growth chambers), assistance from Jan Karlsson in operating the growth chambers, assistance from Prof. Larry Flanagan in calculation of c_c , and financial support from the Knut and Alice Wallenberg Foundation (#2015.0047), VR and the Carl Tryggers Foundation.

LITERATURE CITED

- Ainsworth E.A. & Long S.P. (2005). What have we learned from 15 years of free-air CO₂ enrichment (FACE)? A meta-analytic review of the responses of photosynthesis, canopy properties and plant production to rising CO₂. *New Phytologist* 165(2): 351-371.
- Arp W.J., Van Mierlo J.E.M., Berendse F. & Snijders W. (1998). Interactions between elevated CO₂ concentration, nitrogen and water: effects on growth and water use of six perennial plant species. *Plant Cell and Environment* 21(1): 1-11.
- Belyea L.R. & Malmer N. (2004). Carbon sequestration in peatland: patterns and mechanisms of response to climate change. *Global Change Biology* 10(7): 1043-1052.
- Benjamini Y. & Hochberg Y. (1995). Controlling the false discovery rate: a practical and powerful approach to multiple testing. *Journal of the Royal Statistical Society Series B* 57: 289-300.
- Berendse F., Van Breemen N., Rydin H., Buttler A., Heijmans M., Hoosbeek M.R., Lee J.A., Mitchell E., Saarinen T., Vasander H., *et al.* (2001). Raised atmospheric CO₂ levels and increased N deposition cause

- shifts in plant species composition and production in Sphagnum bogs. *Global Change Biology* 7(5): 591-598.
- Betson T.R., Augusti A. & Schleucher J. (2006). Quantification of deuterium isotopomers of tree-ring cellulose using nuclear magnetic resonance. *Analytical Chemistry* 78(24): 8406-8411.
- Brooks A. & Farquhar G.D. (1985). Effect of temperature on the CO₂/O₂ specificity of ribulose-1,5-bisphosphate carboxylase oxygenase and the rate of respiration in the light - Estimates from gas-exchange measurements on spinach. *Planta* 165(3): 397-406.
- Charman D.J., Beilman D.W., Blaauw M., Booth R.K., Brewer S., Chambers F.M., Christen J.A., Gallego-Sala A., Harrison S.P., Hughes P.D.M., *et al* . (2013). Climate-related changes in peatland carbon accumulation during the last millennium. *Biogeosciences* 10(2): 929-944.
- Cotrufo M.F., Ineson P. & Scott A. (1998). Elevated CO₂ reduces the nitrogen concentration of plant tissues. *Global Change Biology* 4(1): 43-54.
- DeLucia E.H., Moore D.J. & Norby R.J. (2005). Contrasting responses of forest ecosystems to rising atmospheric CO₂: Implications for the global C cycle. *Global Biogeochemical Cycles* 19(3).
- Drake B.G., Gonzalez Meler M.A. & Long S.P. (1997). More efficient plants: A consequence of rising atmospheric CO₂? *Annual Review of Plant Physiology and Plant Molecular Biology* 48: 609-639.
- Ehlers I., Augusti A., Betson T.R., Nilsson M.B., Marshall J.D. & Schleucher J. (2015). Detecting long-term metabolic shifts using isotopomers: CO₂-driven suppression of photorespiration in C₃ plants over the 20th century. *Proceedings of the National Academy of Science* , USA 112(51): 15585-15590.
- Evans J.R. & von Caemmerer S. (2013). Temperature response of carbon isotope discrimination and mesophyll conductance in tobacco. *Plant Cell and Environment* 36(4): 745-756.
- Farquhar G.D., Ehleringer J.R. & Hubick K.T. (1989). Carbon isotope discrimination and photosynthesis. *Annual Review of Plant Physiology and Plant Molecular Biology* 40: 503-537.
- Flanagan L.B. & Farquhar G.D. (2014). Variation in the carbon and oxygen isotope composition of plant biomass and its relationship to water-use efficiency at the leaf- and ecosystem-scales in a northern Great Plains grassland. *Plant Cell and Environment* 37(2): 425-438.
- Franz D., Acosta M., Altimir N., Arriga N., Arrouays D., Aubinet M., Aurela M., Ayres E., López-Ballesteros A., *et al* . (2018). Towards long-term standardized carbon and greenhouse gas observation for monitoring Europe's terrestrial ecosystems: a review. *International Agrophysics* 32(4): 439-455.
- Frolking S., Talbot J., Jones M.C., Treat C.C., Kauffman J.B., Tuittila E.S. & Roulet N. (2011). Peatlands in the Earth's 21st century climate system. *Environmental Reviews* 19: 371-396.
- Gallego-Sala A.V., Charman D.J., Brewer S., Page S.E., Prentice I.C., Friedlingstein P., Moreton S., Amesbury M.J., Beilman D.W., Björck S., *et al* . (2018). Latitudinal limits to the predicted increase of the peatland carbon sink with warming. *Nature Climate Change* 8(10): 907-913.
- Graven H., Allison C.E., Etheridge D.M., Hammer S., Keeling R.F., Levin I., Meijer H.A.J., Rubino M., Tans P.P., Trudinger C.M., *et al* . (2017). Compiled records of carbon isotopes in atmospheric CO₂ for historical simulations in CMIP6. *Geoscientific Model Development* 10(12): 4405-4417.
- Gunnarsson U. (2005). Global patterns of Sphagnum productivity. *Journal of Bryology* 27: 269-279.
- Hajek T., Tuittila E.S., Ilomets M. & Laiho R. (2009). Light responses of mire mosses - a key to survival after water-level drawdown? *Oikos* 118(2): 240-250.
- Harley P.C., Tenhunen J.D., Murray K.J. & Beyers J. (1989). Irradiance and temperature effects on photosynthesis of tussock tundra Sphagnum mosses from the foothills of the Philip Smith Mountains, Alaska. *Oecologia* 79(2): 251-259.

- Hayward P.M. & Clymo R.S. (1982). Profiles of water-content and pore-size in Sphagnum and peat, and their relation to peat bog ecology. *Proceedings of the Royal Society Series B-Biological Sciences* 215(1200): 299-325.
- Heijmans M.M.P.D., Berendse F., Arp W.J., Masselink A.K., Klees H., de Visser W. & van Breemen N. (2001). Effects of elevated carbon dioxide and increased nitrogen deposition on bog vegetation in the Netherlands. *Journal of Ecology* 89(2): 268-279.
- Heijmans M.M.P.D., Klees H., de Visser W. & Berendse F. (2002). Response of a Sphagnum bog plant community to elevated CO₂ and N supply. *Plant Ecology* 162(1): 123-134.
- Hilbert D.W., Roulet N. & Moore T. (2000). Modelling and analysis of peatlands as dynamical systems. *Journal of Ecology* 88(2): 230-242.
- Hogg E.H. (1993). Decay potential of hummock and hollow Sphagnum peats at different depths in a Swedish raised bog. *Oikos* 66(2): 269-278.
- Indermühle A., Stocker T.F., Joos F., Fischer H., Smith H.J., Wahlen M., Deck B., Mastroianni D., Tschumi J., Blunier T., *et al.* (1999). Holocene carbon-cycle dynamics based on CO₂ trapped in ice at Taylor Dome, Antarctica. *Nature* 398(6723): 121-126.
- IPCC. (2013). Stocker T.F. *et al.*, eds. Climate Change 2013: The Physical Science Basis. Contribution of Working Group I to the Fifth Assessment Report of the Intergovernmental Panel on Climate Change. Cambridge University Press, Cambridge, UK.
- Jauhiainen J., Vasander H. & Silvola J. (1994). Response of Sphagnum fuscum to N deposition and increased CO₂. *Journal of Bryology* 118: 83-96.
- Jauhiainen J., Vasander H. & Silvola J. (1998). Nutrient concentration in Sphagnum at increased N-deposition rates and raised atmospheric CO₂ concentrations. *Plant Ecology* 138(2): 149-160.
- Jauhiainen J. & Silvola J. (1999). Photosynthesis of Sphagnum fuscum at long-term raised CO₂ concentrations. *Annales Botanici Fennici* 36(1): 11-19.
- Kirschbaum M.U.F. (2011). Does enhanced photosynthesis enhance growth? Lessons learned from CO₂ enrichment studies. *Plant Physiology* 155(1): 117-124.
- Klinggräff H.V. (1872). Sphagnum fuscum. *Schriften Königl. Phys.-Ökon. Ges. Königsberg*, 13(1): 4, 4.
- Laine A.M., Juurola E., Hajek T. & Tuittila E.S. (2011). Sphagnum growth and ecophysiology during mire succession. *Oecologia* 167(4): 1115-1125.
- Laing W.A., Ogren W.L. & Hageman R.H. (1974). Regulation of soybean net photosynthetic CO₂ fixation by interaction of CO₂, O₂, and ribulose 1,5-diphosphate carboxylase. *Plant Physiology* 54(5): 678-685.
- Laing C.G., Granath G., Belyea L.R., Allton K.E. & Rydin H. (2014). Tradeoffs and scaling of functional traits in Sphagnum as drivers of carbon cycling in peatlands. *Oikos* 123(7): 817-828.
- Limpens J., Berendse F., Blodau C., Canadell J.G., Freeman C., Holden J., Roulet N., Rydin H. & Schaepman-Strub G. (2008). Peatlands and the carbon cycle: from local processes to global implications - a synthesis. *Biogeosciences* 5(5): 1475-1491.
- Loisel J., Yu Z.C., Beilman D.W., Camill P., Alm J., Amesbury M.J., Anderson D., Andersson S., Bochicchio C., Barber K., *et al.* (2014). A database and synthesis of northern peatland soil properties and Holocene carbon and nitrogen accumulation. *Holocene* 24(9): 1028-1042.
- McCarter C.P.R. & Price J.S. (2014). Ecohydrology of Sphagnum moss hummocks: mechanisms of capitula water supply and simulated effects of evaporation. *Ecohydrology* 7(1): 33-44.

- Mitchell E.A.D., Buttler A., Grosvernier P., Rydin H., Siegenthaler A. & Gobat J.M. (2002). Contrasted effects of increased N and CO₂ supply on two keystone species in peatland restoration and implications for global change. *Journal of Ecology* 90(3): 529-533.
- Moor H., Rydin H., Hylander K., Nilsson M.B., Lindborg R. & Norberg J. (2017). Towards a trait-based ecology of wetland vegetation. *Journal of Ecology* 105(6): 1623-1635.
- Nijp J.J., Limpens J., Metselaar K., van der Zee S.E.A.T.M., Berendse F. & Robroek B.J.M. (2014). Can frequent precipitation moderate the impact of drought on peatmoss carbon uptake in northern peatlands? *New Phytologist* 203(1): 70-80.
- Nijp J.J., Metselaar K., Limpens J., Teutschbein C., Peichl M., Nilsson M.B., Berendse F. & van der Zee S.E.A.T.M. (2017). Including hydrological self-regulating processes in peatland models: Effects on peatmoss drought projections. *Science of the Total Environment* 580: 1389-1400.
- Peichl M., Oquist M., Lofvenius M.O., Ilstedt U., Sagerfors J., Grelle A., Lindroth A. & Nilsson M.B. (2014). A 12-year record reveals pre-growing season temperature and water table level threshold effects on the net carbon dioxide exchange in a boreal fen. *Environmental Research Letters* 9(5).
- Price J.S. & Whittington P.N. (2010). Water flow in Sphagnum hummocks: Mesocosm measurements and modelling. *Journal of Hydrology* 381(3-4): 333-340.
- Pugh T.A.M., Muller C., Arneth A., Haverd V. & Smith B. (2016). Key knowledge and data gaps in modelling the influence of CO₂ concentration on the terrestrial carbon sink. *Journal of Plant Physiology* 203: 3-15.
- Poorter H. (1998). Do slow-growing species and nutrient-stressed plants respond relatively strongly to elevated CO₂? *Global Change Biology* 4(6): 693-697.
- Rice S.K. & Giles L. (1996). The influence of water content and leaf anatomy on carbon isotope discrimination and photosynthesis in Sphagnum. *Plant, Cell and Environment* 19: 118-124.
- Rydin H. & Clymo R.S. (1989). Transport of carbon and phosphorus-compounds about Sphagnum. *Proceedings of the Royal Society Series B-Biological Sciences* 237(1286): 63-84.
- Rydin H., Gunnarsson U. & Sundberg S. (2006). The role of Sphagnum in peatland development and persistence. In: *Boreal Peatland Ecosystems* (eds. Wieder R.K. & Vitt D.H.). Ecological Studies (Analysis and Synthesis), vol 188. Springer, Berlin, Heidelberg.
- Rydin H. & Jeglum J.K. (2013). *The Biology of Peatlands*, 2nd edition. Oxford, UK: Oxford University Press.
- Schimel D., Stephens B.B. & Fisher J.B. (2015). Effect of increasing CO₂ on the terrestrial carbon cycle. *Proceedings of the National Academy of Science*, USA 112(2): 436-441.
- Schipperges B. & Rydin H. (1998). Response of photosynthesis of Sphagnum species from contrasting microhabitats to tissue water content and repeated desiccation. *New Phytologist* 140(4): 677-684.
- Schleucher J., Vanderveer P., Markley J.L. & Sharkey T.D. (1999). Intramolecular deuterium distributions reveal disequilibrium of chloroplast phosphoglucose isomerase. *Plant Cell and Environment* 22(5): 525-533.
- Silvola J. & Aaltonen H. (1984). Water content and photosynthesis in the peat mosses Sphagnum fuscum and S. angustifolium. *Annales Botanici Fennici* 21: 1-6.
- Steel R., Torri J. & Dickey D. (1997). *Principles and Procedures of Statistics: A Biometrical Approach*. McGraw-Hill College.
- Titus J.E., Wagner D.J. & Stephens M.D. (1983). Contrasting water relations of photosynthesis for 2 Sphagnum mosses. *Ecology* 64(5): 1109-1115.
- Titus J.E. & Wagner D.J. (1984). Carbon balance for two Sphagnum mosses - Water-balance resolves a physiological paradox. *Ecology* 65(6): 1765-1774.

Toet S., Cornelissen J.H.C., Aerts R., van Logtestijn R.S.P., de Beus M. & Stoevelaar R. (2006). Moss responses to elevated CO₂ and variation in hydrology in a temperate lowland peatland. *Plant Ecology* 182(1-2): 27-40.

van der Heijden E., Jauhiainen J., Silvola J., Vasander H. & Kuiper P.J.C. (2000a). Effects of elevated atmospheric CO₂ concentration and increased nitrogen deposition on growth and chemical composition of ombrotrophic *Sphagnum balticum* and oligo-mesotrophic *Sphagnum papillosum*. *Journal of Bryology* 22: 175-182.

van der Heijden E., Verbeek S.K. & Kuiper P.J.C. (2000b). Elevated atmospheric CO₂ and increased nitrogen deposition: effects on C and N metabolism and growth of the peat moss *Sphagnum recurvum* P. Beauv. var. *mucronatum* (Russ.) Warnst. *Global Change Biology* 6(2): 201-212.

Venables W.N. & Ripley B.D. (2002). *Modern Applied Statistics with S*, 4th edition. New York: Springer.

Werner R.A., Bruch B.A. & Brand W.A. (1999). ConFlo III - An interface for high precision $\delta^{13}\text{C}$ and $\delta^{15}\text{N}$ analysis with an extended dynamic range. *Rapid Communications in Mass Spectrometry* 13(13): 1237-1241.

Weston D.J., Timm C.M., Walker A.P., Gu L.H., Muchero W., Schmutz J., Shaw A.J., Tuskan G.A., Warren J.M. & Wullschlegel S.D. (2015). *Sphagnum* physiology in the context of changing climate: emergent influences of genomics, modelling and host-microbiome interactions on understanding ecosystem function. *Plant Cell and Environment* 38(9): 1737-1751.

Williams T.G. & Flanagan L.B. (1996). Effect of changes in water content on photosynthesis, transpiration and discrimination against $^{13}\text{CO}_2$ and $\text{C}^{18}\text{O}^{16}\text{O}$ in *Pleurozium* and *Sphagnum*. *Oecologia* 108(1): 38-46.

Williams T.G. & Flanagan L.B. (1998). Measuring and modelling environmental influences on photosynthetic gas exchange in *Sphagnum* and *Pleurozium*. *Plant Cell and Environment* 21(6): 555-564.

Wu J.H., Roulet N.T., Nilsson M., Lafleur P. & Humphreys E. (2012). Simulating the carbon cycling of Northern peat lands using a land surface scheme coupled to a Wetland Carbon Model (CLASS3W-MWM). *Atmosphere-Ocean* 50(4): 487-506.

Wu J.H. & Roulet N.T. (2014). Climate change reduces the capacity of northern peatlands to absorb the atmospheric carbon dioxide: The different responses of bogs and fens. *Global Biogeochemical Cycles* 27: 1005-1024.

Yu Z., Beilman D.W. & Jones M.C. (2009). Sensitivity of northern peatland carbon dynamics to Holocene climate change. In: *Carbon Cycling in Northern Peatlands* (eds. Baird A.J., et al.), Geophys. Monogr. Ser., vol. 184, AGU, Washington, D.C., 55– 69.

TABLES

Table 1. Summary of 4-way ANOVA models of effects of CO₂, temperature (T), water table (WT), light intensity (LI) and their interactions on the measured physiological response variables.

Response vari- able	Main fac- tors	Main fac- tors	Main fac- tors	Main fac- tors	Factor in- ter- ac- tions	Factor in- ter- ac- tions	Factor in- ter- ac- tions	Factor in- ter- ac- tions	Factor in- ter- ac- tions	Model p.	
	CO ₂	T	WT	LI	CO ₂ x T	CO ₂ x WT	CO ₂ x LI	WT x T	WT x LI	R ²	
D6^S/D6^RP ratio	<0.001	0.004	<0.001	<i>n.s.</i>	<i>n.s.</i>	0.005	<i>n.s.</i>	<i>n.s.</i>	<i>n.s.</i>	0.77	4
<i>F</i>	19.0	9.8	64.5			9.4					

Response variable		Main factors	Main factors	Main factors	Main factors	Factor in-ter-ac-tions	Factor in-ter-ac-tions	Factor in-ter-ac-tions	Factor in-ter-ac-tions	Factor in-ter-ac-tions	Model p.	
Biomass production	<i>P</i>	<i>n.s.</i>	<0.001	<0.001	0.003	<i>n.s.</i>	<i>n.s.</i>	<i>n.s.</i>	0.005	0.047	0.88	5
$\delta^{13}\text{C}$	<i>F</i>		69.4	131.6	10.7				9.0	4.3		5
	<i>P</i>	<0.001	<0.001	<0.001	0.020	<i>n.s.</i>	<0.001	<i>n.s.</i>	<i>n.s.</i>	<i>n.s.</i>	0.84	5
	<i>F</i>	23.2	17.6	88.8	6.0		19.3					5
c_c / c_a	<i>P</i>	0.046	0.035	<0.001	0.022	<i>n.s.</i>	<0.001	<i>n.s.</i>	<i>n.s.</i>	<i>n.s.</i>	0.80	5
C/N ratio	<i>F</i>	4.3	4.9	86.3	5.8		18.8					6
	<i>P</i>	0.003	0.083	<0.001	<i>n.s.</i>	0.074	0.022	<i>n.s.</i>	0.004	<i>n.s.</i>	0.68	6
N content	<i>F</i>	10.9	3.2	27.5		3.4	5.9		9.5			7
	<i>P</i>	0.013	<i>n.s.</i>	<0.001	<i>n.s.</i>	<i>n.s.</i>	0.070	<i>n.s.</i>	0.031	<i>n.s.</i>	0.58	7
Biomass density	<i>F</i>	7.1		19.6			3.5		5.1			6
	<i>P</i>	<i>n.s.</i>	<i>n.s.</i>	<0.001	<0.001	<i>n.s.</i>	<i>n.s.</i>	<i>n.s.</i>	0.097	<0.001	0.93	6
Height increment	<i>F</i>			180.5	137.6				2.9	54.9		8
	<i>P</i>	0.084	<0.001	<i>n.s.</i>	<0.001	0.020	<i>n.s.</i>	0.035	0.042	0.017	0.88	8
	<i>F</i>	3.2	109.7		51.1	6.2		4.9	4.6	6.5		

Note that 3- and 4-way interactions were excluded from the models. Non-significant factors/interactions with $P > 0.1$ are denoted as *n.s.*. *df*, degrees of freedom of the model and residuals.

Table 2 . Summary of 2-way ANOVA models of effects of CO₂ and water table (WT) and their interaction on the measured physiological response variables of *S. majus* .

Response variable	Response variable	CO ₂	WT	CO ₂ x WT	R ² <i>df</i>
D6 ^S /D6 ^R ratio	<i>P</i>	0.071	<0.001	<i>n.s.</i>	0.88 2/9
Biomass production	<i>F</i>	4.19	62.16		
	<i>P</i>	<i>n.s.</i>	0.01	<i>n.s.</i>	0.54 1/10
Biomass density	<i>F</i>		10.63		
	<i>P</i>	0.048	0.008	0.057	0.74 3/8
Height increment	<i>F</i>	5.46	12.4	4.93	
	<i>P</i>	0.012	<i>n.s.</i>	<i>n.s.</i>	0.57 1/10

Response variable	Response variable	CO ₂	WT	CO ₂ x WT	R ² df
	<i>F</i>	10.58			

Non-significant factors/interactions with $P > 0.1$ are denoted as *n.s.*. *df*, degrees of freedom of the model and residuals.

FIGURE LEGENDS

Fig. 1 . Deuterium NMR spectrum of glucose derived from structural carbohydrates of *S. fuscum* . The integral of each peak is proportional to the abundance of the deuterium (D) isotopomers at the corresponding position in the glucose molecule (H1 – H6). The ratio of the isotopomer abundance of D6^S and D6^R corresponds to the photorespiration/photosynthesis ratio (Ehlers *et al.* , 2015).

Fig. 2 . D6^S /D6^R ratios and biomass production of *S. fuscum* incubated in the growth chambers at indicated atmospheric CO₂, temperature, water table (WT) and light intensity settings. Solid and striped bars indicate low and high atmospheric CO₂, respectively. LT and HT indicate low and high temperature, and LL and HL low and high light, respectively. (A) D6^S /D6^R isotopomer ratios reflecting the photorespiration/photosynthesis ratio and (B) daily biomass production during the two-month incubation period. Error bars indicate \pm SE, $n = 3$. Different letters above error bars indicate significant differences ($P < 0.05$) according to Fisher's least significant difference post-hoc test with Benjamini-Hochberg correction.

Fig. 3 . Physiological response variables of *S. fuscum* incubated in the growth chambers at indicated atmospheric CO₂, temperature, water table (WT) and light intensity settings. Solid and striped bars indicate low and high atmospheric CO₂, respectively. LT and HT indicate low and high temperature, and LL and HL low and high light, respectively. (A) whole-tissue $\delta^{13}\text{C}$ values and (B) chloroplastic to ambient CO₂ (c_c/c_a) ratios, (C) whole-tissue C/N ratio and (D) N contents, (E) biomass density in total biomass dry weight per unit volume and (F) moss height increment. Error bars indicate \pm SE, $n = 3$. Different letters above error bars indicate significant differences ($P < 0.05$) according to Fisher's least significant difference post-hoc test with Benjamini-Hochberg correction.

Fig. 4 . D6^S /D6^R ratios, biomass production, density and height increment of *S. majus* incubated in the growth chambers at indicated atmospheric CO₂ and water table (WT) settings. Data were obtained for the high temperature and low light treatment. Solid and striped bars indicate low and high atmospheric CO₂, respectively. (A) D6^S /D6^R isotopomer ratios reflecting the photorespiration/photosynthesis ratio, (B) daily biomass production during the two-month incubation period, (C) biomass density in total biomass dry weight per unit volume and (D) moss height increment. Error bars indicate \pm SE, $n = 3$. Different letters above error bars indicate significant differences ($P < 0.05$) according to student's t-test.

SUPPLEMENTAL DATA

Supplemental Fig. S1. Experimental setup of the incubation of *S. fuscum* and *S. majus* mesocosms in climate growth chambers.

Supplemental Fig. S2. Time course of *S. fuscum* and *S. majus* height increment during the incubation period.

Supplemental Fig. S3. Tissue water content, C content, CO₂ diffusion gradient ($c_a - c_c$) and ¹⁵N discrimination of *S. fuscum* incubated in growth chambers.

Supplemental Table S1 . Summary of results of separate 3-way ANOVA models of effects of CO₂, temperature (T), light intensity (LI) and their interactions on the measured response variables listed in Table 1 obtained using the low and high water table (WT) datasets.

Supplemental Table S2 . Summary of the 4-way ANOVA models of effects of CO₂, temperature (T), water table (WT), light intensity (LI) and their interactions on response variables shown in Fig. S3.

Fig. 1

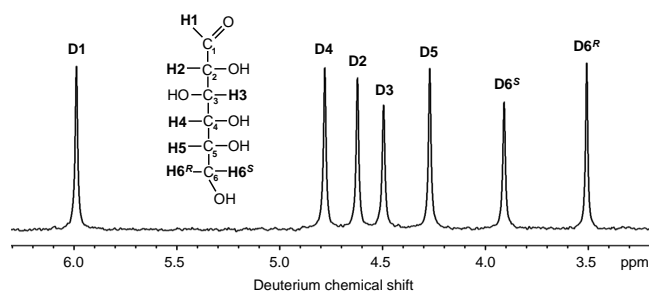


Fig. 2

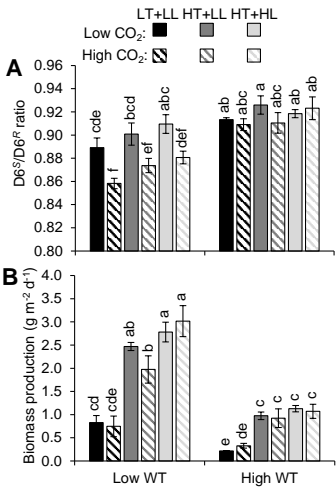


Fig. 3

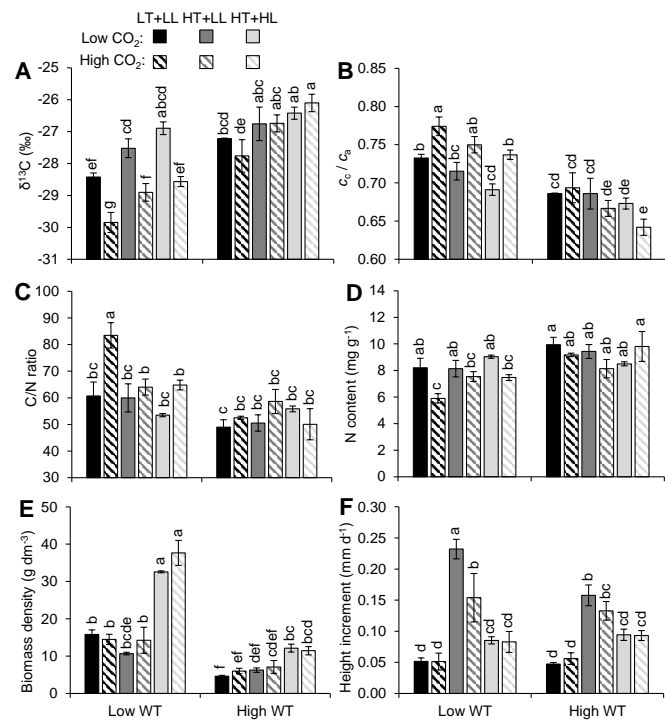


Fig. 4

